

Excitation spectrum of the homogeneous spin liquid

R. Eder

Institut für Theoretische Physik, Universität Würzburg, Am Hubland, 97074 Würzburg, Germany
(July 30, 2018)

We discuss the excitation spectrum of a disordered, isotropic and translationally invariant spin state in the 2D Heisenberg antiferromagnet. The starting point is the nearest-neighbor RVB state which plays the role of the vacuum of the theory, in a similar sense as the Néel state is the vacuum for antiferromagnetic spin wave theory. We discuss the elementary excitations of this state and show that these are not Fermionic spin-1/2 ‘spinons’ but spin-1 excited dimers which must be modeled by bond Bosons. We derive an effective Hamiltonian describing the excited dimers which is formally analogous to spin wave theory. Condensation of the bond-Bosons at zero temperature into the state with momentum (π, π) is shown to be equivalent to antiferromagnetic ordering. The latter is a key ingredient for a microscopic interpretation of Zhang’s SO(5) theory of cuprate superconductivity.

75.10.Jm,75.30.Ds,74.20.Mn,74.72.-h

I. INTRODUCTION

High-temperature superconductivity occurs in a state which is frequently referred to as an ‘RVB spin liquid’. This state has no magnetic order, but strong short range antiferromagnetic correlations. Undoubtedly the strong repulsion between electrons, which turns the system into a charge-transfer insulator at half-filling persists in the doped case, so that a description in terms of free-electron like Slater-determinants is not really adequate. The problem then is, how to describe such a state theoretically. Despite its frequently being referred to in the literature, the RVB spin liquid is a rather elusive concept. For example the precise nature of its ground state and low lying elementary excitations is not known to any degree of certainty. In the following we want to address this problem by studying a disordered state for the 2D Heisenberg antiferromagnet

$$H = J \sum_{\langle i,j \rangle} \mathbf{S}_i \cdot \mathbf{S}_j$$

on a 2D square lattice. Here \mathbf{S}_i denotes a spin 1/2 operator on site i . One might expect that this is a kind of stepping stone also for the doped case, in that the elementary excitations of the undoped spin liquid persist to some degree also for finite doping. Perhaps the best-defined RVB spin liquid is the nearest neighbor RVB state [1–4] - at least this wave function can be written down in compact form. We define the singlet generation operator on the bond i, j

$$s_{i,j}^\dagger = \frac{1}{\sqrt{2}} (\hat{c}_{i,\uparrow}^\dagger \hat{c}_{j,\downarrow}^\dagger - \hat{c}_{i,\downarrow}^\dagger \hat{c}_{j,\uparrow}^\dagger), \quad (1)$$

where $\hat{c}_{i,\sigma}^\dagger = c_{i,\sigma}^\dagger c_{i,\bar{\sigma}} c_{i,\bar{\sigma}}^\dagger$, are the constrained Fermion operators, which do not allow the creation of a second electron on an already singly occupied site. Introducing the operator

$$S = \sum_i (s_{i,i+\hat{x}}^\dagger + s_{i,i+\hat{y}}^\dagger), \quad (2)$$

where e.g. $i + \hat{x}$ denotes the nearest neighbor of site i in x -direction, the nearest neighbor RVB state on a 2D square lattice with $2N$ sites can be written as

$$|RVB\rangle = \frac{1}{\sqrt{n}} \frac{S^N}{N!} |0\rangle, \quad (3)$$

where n is a normalization factor. It corresponds to a superposition of all states which can be obtained by covering the plane compactly with nearest neighbor singlets, all with equal phase. Covering the plane with singlets is equivalent to covering it with dimers, a well-known problem from statistical mechanics [5]. We can therefore rewrite the state as

$$|RVB\rangle = \frac{1}{\sqrt{n}} \sum_a |\psi_a\rangle, \quad (4)$$

where a denotes a dimer covering of the lattice and $|\psi_a\rangle$ the state obtained by putting singlets onto the dimers of a .

In the following, we want to examine the problem of the possible elementary excitations of such a singlet background, and set up an effective Hamiltonian governing their dynamics. The idea of ‘expanding’ around a suitably chosen vacuum state is realized in simplest form in linear spin wave theory. The general line of thought here is quite analogous to linear spin wave theory, with the sole exception that the role of the vacuum (which determines the symmetries of the ground state) is played by the ‘singlet soup’ (3) instead of the Néel state. A similar approach has previously been applied to dimerized planar Heisenberg-type models [6,7] to spin ladders [8,9], to strongly coupled Heisenberg planes [10,11], and to Spin-Peierls-like spin chains [12,13]. An example where the fluctuations are Fermionic rather than Bosonic in nature

is provided by the Kondo lattice [14]. The main difference as compared to the present work is that in all of these works a rather unique and simple dimer covering of the system is given by the topology or the form of the Hamiltonian - the complications that arise from the use of a disordered ‘singlet soup’ such as (3) then can be avoided.

While the technical complications arising from the use of a dimer basis are considerable, this approach also has some major advantages: in a site basis it is virtually impossible to even write down a disordered spin state, because one has to deal with the spin degeneracy on each single site. The calculation only becomes feasible if this site-degeneracy is lifted, for example by assuming strict Néel order as in spin wave theory. On the other hand, the degeneracy is automatically taken care of in the dimer basis, because two interacting sites do have a unique ground state. A further considerable advantage of the dimer basis is, that it is easily enlarged by hole pairs on nearest neighbors, so as to describe a superconducting state. Indeed, as will be seen below, the present description of the antiferromagnetic phase most naturally can be generalized to comprise also a superconducting phase, thereby providing a very simple microscopical picture for the SO(5) rotations which smoothly connect antiferromagnetic and superconducting phase in Zhang’s theory [15] of cuprate superconductors.

II. ELEMENTARY EXCITATIONS OF A ‘SINGLET SOUP’

The nearest neighbor-RVB state (4) has the symmetry properties expected for a homogeneous spin liquid: it is isotropic, translationally invariant, is an exact spin singlet and has no magnetic order. On the other hand, just as the Néel state, it is not an eigenstate of H . If we take one singlet configuration $|\psi_a\rangle$ and act with the exchange term on a bond connecting two different singlets (see Figure 1a) we can create a state which no longer can be represented as a superposition of only nearest neighbor singlets. Such a state therefore represents a kind of fluctuation and as a first step we need to understand the character of these fluctuations. It might appear [16] that the energetically most favorable fluctuation is the state shown in Figure 1b: two nearest neighbor singlets are transformed into a configuration with only one nearest neighbor singlet and a second singlet connecting more distant sites. Nominally the energy increases by only $3J/4$ in this transition, because the only change is the loss of one nearest neighbor singlet. Because singlet and triplet are degenerate for sites which are not connected by an exchange bond, we might as well consider the two spins connected by the ‘long singlet’ as being unpaired (see Figure 1c). The transition from Figure 1 a→b could thus be viewed as pair creation of two unpaired spins.

Next, by acting with the exchange term on a bond which connects a dangling spin to another singlet (see Figure 1c), we can recouple the spins so as to form a new singlet and leave one of the formerly paired spins unpaired (see Figure 1d). This process corresponds to a propagation

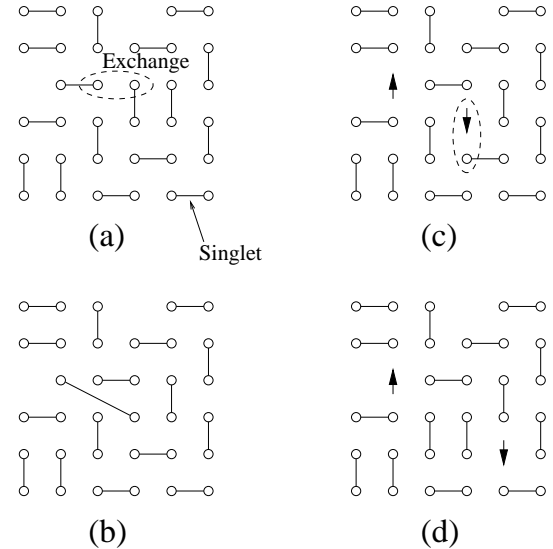


FIG. 1. An incorrect picture for fluctuations in a singlet background.

of the dangling spin. We would thus arrive at the conclusion that the fluctuations out of the nearest neighbor RVB state are unpaired spins, which carry a spin of $1/2$ and consequently must obey Fermi statistics. Clearly, these excitations should be identified with the ominous ‘spinons’.

Further reasoning shows, however, that the line of thought leading to the introduction of the ‘spinons’ misses a small but crucial detail. The first reason is that the state in Figure 1b is not orthogonal to the vacuum,

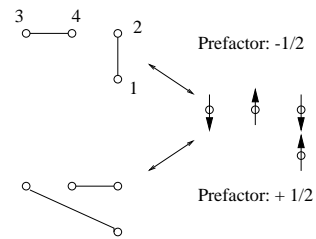


FIG. 2. Placing singlets in either of the two ways shown on the left produces the spin configuration on the right with the indicated prefactors. This gives a contribution of $-1/4$ to the overlap, an equal contribution comes from the spin reversed configuration.

and thus cannot represent a true fluctuation. More precisely, if we introduce (see Figures 1 and 2))

$$|a\rangle = s_{1,2}^\dagger s_{3,4}^\dagger |0\rangle,$$

$$|b\rangle = s_{1,3}^\dagger s_{4,2}^\dagger |0\rangle,$$

it is straightforward to see (Figure 2) that $\langle a|b\rangle = -\frac{1}{2}$, in other words: after the ‘transition’ Figure 1a→b we remain in the original state, Figure 1a, with a probability of 25%. The problem of non-orthogonality is not restricted to the first step in Figure 1: the states Fig. 1c and 1d have an overlap of 1/2, and this generalizes to any two states which differ by one hopping process of a ‘spinon’. The non-orthogonality problem thus is omnipresent and severe.

Let us therefore return to the first step, Figure 1 a→b, and consider how we can remedy the problem. The most natural way to proceed is to form the orthogonal complement

$$|b'\rangle = |b\rangle - \langle a|b\rangle |a\rangle,$$

so as to see ‘what is really new’ in the state $|b\rangle$. A straightforward computation shows that after normalization to unity the orthogonal complement is

$$|b'\rangle = \frac{1}{\sqrt{3}} \sum_{\alpha=x,y,z} t_{12,\alpha}^\dagger t_{34,\alpha}^\dagger |0\rangle. \quad (5)$$

Here we have introduced the operators [17,6]

$$\begin{aligned} t_{ij,x}^\dagger &= \frac{-1}{\sqrt{2}} (\hat{c}_{i,\uparrow}^\dagger \hat{c}_{j,\uparrow}^\dagger - \hat{c}_{i,\downarrow}^\dagger \hat{c}_{j,\downarrow}^\dagger), \\ t_{ij,y}^\dagger &= \frac{i}{\sqrt{2}} (\hat{c}_{i,\uparrow}^\dagger \hat{c}_{j,\uparrow}^\dagger + \hat{c}_{i,\downarrow}^\dagger \hat{c}_{j,\downarrow}^\dagger), \\ t_{ij,z}^\dagger &= \frac{1}{\sqrt{2}} (\hat{c}_{i,\uparrow}^\dagger \hat{c}_{j,\downarrow}^\dagger + \hat{c}_{i,\downarrow}^\dagger \hat{c}_{j,\uparrow}^\dagger), \end{aligned} \quad (6)$$

which create the three components of the *triplet* on the bond (i,j) . We arrive at the conclusion that the true fluctuation out of the nearest neighbor singlet background is not the creation of two Fermionic ‘spinons’, but rather the creation of two excited dimers, which carry a spin of 1 and consequently should be modeled by bond-Bosons [17,6]. The further evolution of the created triplets then is quite obvious (see Figure 3) (but completely different from that of the ‘spinons’): by exchange along bonds connecting the triplets with neighboring singlets the triplets can de-excite while simultaneously the singlet turns into a triplet - this process, which is very much reminiscent of the propagation of a Frenkel-type exciton corresponds to the propagation of the excited dimer. Note that unlike the ‘spinon’ states in Figure 1, all different states in Figure 3 are mutually rigorously orthogonal. As a matter of fact there are problems with non-orthogonalities also for the triplet states - these are ‘inherited’ from the original nearest neighbor RVB state. They will be discussed in detail below and be shown to be much less severe than those for the ‘spinon’ states. Their main effect is to replace the simple excited dimer by a more delocalized object, which

resonates between different orientations within a limited spatial region.

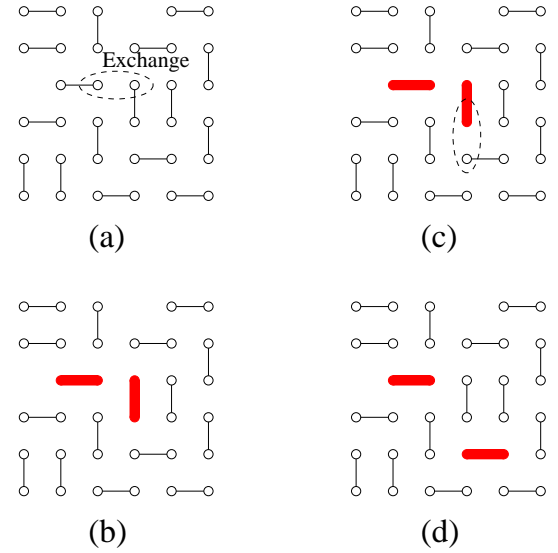


FIG. 3. A more correct picture for fluctuations in a singlet background.

To be more precise, we now discuss the action of the Heisenberg exchange on all possible configurations of nearest neighbor singlets and triplets. Consider two *nearest neighbor bonds* (i,j) and (i',j') , and assume that they are connected by a single bond (i,i') . Denoting the Heisenberg exchange along the latter bond by $h_{i,i'}$ we have:

$$\begin{aligned} h_{i,i'} s_{i,j}^\dagger s_{i',j'}^\dagger &= \frac{J}{4} \mathbf{t}_{i,j}^\dagger \cdot \mathbf{t}_{i',j'}^\dagger, \\ h_{i,i'} s_{i,j}^\dagger t_{i',j'}^\dagger &= \frac{J}{4} \mathbf{t}_{i,j}^\dagger s_{i',j'}^\dagger - \frac{iJ}{4} \mathbf{t}_{i,j}^\dagger \times \mathbf{t}_{i',j'}^\dagger, \\ h_{i,i'} t_{i,j,\alpha}^\dagger t_{i',j',\alpha}^\dagger &= \frac{J}{4} s_{i,j}^\dagger s_{i',j'}^\dagger \\ &\quad - \frac{J}{4} (\mathbf{t}_{i,j}^\dagger \cdot \mathbf{t}_{i',j'}^\dagger - t_{i,j,\alpha}^\dagger t_{i',j',\alpha}^\dagger), \\ h_{i,i'} t_{i,j,\alpha}^\dagger t_{i',j',\beta}^\dagger &= \frac{J}{4} t_{i,j,\beta}^\dagger t_{i',j',\alpha}^\dagger \\ &\quad - \frac{iJ\epsilon_{\alpha\beta\gamma}}{4} (t_{i,j,\gamma}^\dagger s_{i',j'}^\dagger - s_{i,j}^\dagger t_{i',j',\gamma}^\dagger). \end{aligned} \quad (7)$$

These equations show that if we start out from states containing nearest neighbor singlets or triplets on the l.h.s., the exchange term only produces states which again consist of nearest neighbor singlets or triplets on the r.h.s (had the two bonds been connected by exchange along another bond, (j,i') , (i,j') or (j,j') , we would have obtained the same equations with the sole difference that in some cases the prefactors change their sign). This proves rigorously that acting with an arbitrarily high power of the Hamiltonian onto the nearest neighbor RVB state produces only states which can be built up from *nearest*

neighbor singlets or triplets.

This ‘theorem’ in fact holds true in a more general sense: on a single dimer m , the 4 states s_m^\dagger and t_m^\dagger do form a complete basis [6]. Thus, if we use a fixed dimer covering a , the set of states obtained by placing singlets and triplets on the dimers of a form a complete basis of the Hilbert space. Adding up such states obtained from *all possible* dimer coverings then clearly produces a highly overcomplete basis of the Hilbert space, which therefore must automatically include states with singlets of arbitrary length. It follows that all states with longer-range singlets also can be represented as superpositions of states which are composed exclusively from nearest-neighbor singlets and triplets. These states are therefore redundant, and if we formulate a self-consistent theory in terms of nearest-neighbor singlets and triplets, we have automatically included these longer-ranged singlets. The fact that we are using a nearest-neighbor RVB state as the starting point for constructing our theory therefore means no loss of generality and in particular does by no means imply that we are considering only states with only very short-ranged antiferromagnetic correlations. In fact, it will be shown below that one can construct even states with infinite-range antiferromagnetic order by using exclusively nearest neighbor singlets and triplets.

The preceding considerations suggest that we should model the excitation spectrum of the nearest neighbor singlet vacuum by Bosonic excitations, which approximately correspond to excited dimers. Assuming that the bonds in the system have been labeled in some way, we denote the triplet operator on bond i by t_i^\dagger . Then, we introduce the following basis states

$$|\Psi_{i_1\alpha_1, i_2\alpha_2, \dots, i_m\alpha_m}\rangle = \frac{1}{\sqrt{n(i_1\alpha_1, i_2\alpha_2, \dots, i_m\alpha_m)}} \frac{S^{N-m}}{(N-m)!} \prod_{\nu=1}^m t_{i_\nu, \alpha_\nu}^\dagger |0\rangle, \quad (8)$$

where $n(i_1\alpha_1, i_2\alpha_2, \dots, i_m\alpha_m)$ is a normalization factor. They describe a certain number (m) of triplets which are ‘immersed into the singlet soup’. Thereby the singlets fill the space in between the triplets compactly in all possible ways. All states which can be generated by pair creation and propagation of triplet bonds (such as the ones shown in Figure 3) can be represented in this way. We next consider the triplets as Boson-like elementary excitations of the singlet-background, in precisely the same way as misaligned spins are considered as Bosonic excitations in a ‘Néel background’ in antiferromagnetic spin wave theory. Re-interpreting the state

$$|\psi_{i_1\alpha_1, i_2\alpha_2, \dots, i_m\alpha_m}\rangle \rightarrow \prod_{\nu=1}^m \tau_{i_\nu, \alpha_\nu}^\dagger |0\rangle,$$

where the $\tau_{i_\nu, \alpha_\nu}^\dagger$ represent Boson operators, we may expect to describe the dynamics of these Bosons by a Hamiltonian of the form [18]

$$H = J \sum_i \boldsymbol{\tau}_i^\dagger \cdot \boldsymbol{\tau}_i + \sum_{i,j} (\Delta_{ij} \boldsymbol{\tau}_i^\dagger \cdot \boldsymbol{\tau}_j^\dagger + H.c.) + \sum_{i,j} \epsilon_{ij} \boldsymbol{\tau}_i^\dagger \cdot \boldsymbol{\tau}_j, \quad (9)$$

where we have grouped the three triplet components into a 3-vector $\boldsymbol{\tau}$ so as to stress manifest rotation invariance. The first term in (9) corresponds to the energy of formation of the triplets, the second term describes pair creation processes as in Figure 3a → 3b, and the third term accounts for the propagation of the triplets, see Figure 3c → 3d. The matrix elements ϵ_{ij} and Δ_{ij} should be obtained by computing matrix elements of the Heisenberg Hamiltonian H between the corresponding states (8). Of course one thereby has to assume that for example the matrix element for a triplet jumping from bond m to bond n does not depend significantly on the positions of the other triplets - otherwise a description in terms of a single-particle like Hamiltonian would not be feasible. As is the case in spin wave theory, the τ -Bosons have to obey a hard-core constraint, and in fact presence of one Boson prohibits the presence of another Boson not only on the same bond, but also on all bonds which share a site with the original one.

In the following, we will first study the problem of a single excited dimer in the singlet background, in other words we want to compute the ‘bare’ Boson dispersion $\epsilon(\mathbf{k})$ in (9). As our basis states we consequently choose (suppressing the x y or z spin-index of the triplet):

$$|i, \alpha\rangle = \frac{1}{\sqrt{n_1}} \frac{S^{N-1}}{(N-1)!} t_{i, i+\hat{\alpha}}^\dagger |0\rangle, \quad (10)$$

where $\alpha=x, y$ denotes the direction of the bond in real space, and n_1 a normalization factor. In this state one triplet is put onto the bond $(i, i+\hat{\alpha})$ and the remainder of the lattice is covered compactly by singlets in all possible ways. Next, we introduce the Fourier transforms

$$|\mathbf{k}, \alpha\rangle = \frac{e^{i\mathbf{k}_\alpha/2}}{\sqrt{2N}} \sum_j |j, \alpha\rangle e^{i\mathbf{k} \cdot \mathbf{R}_j}. \quad (11)$$

In the Hilbert space of bond-Bosons, this state would be denoted by $\tilde{\tau}_{\mathbf{k}, \alpha}^\dagger |0\rangle$. The procedure to be followed then is like this: in a first step we compute the 2×2 overlap matrix $N(\mathbf{k}) = \langle \tilde{\tau}_{\mathbf{k}, \alpha} \tilde{\tau}_{\mathbf{k}, \alpha}^\dagger \rangle$ and diagonalize it. Denoting the resulting eigenvectors and eigenvalues by \mathbf{e}_ν and λ_ν , the states

$$\tau_{\mathbf{k}, \nu}^\dagger |0\rangle = \frac{1}{\sqrt{\lambda_\nu}} \sum_{\alpha=x, y} \mathbf{e}_{\nu, \alpha} \tilde{\tau}_{\mathbf{k}, \alpha}^\dagger |0\rangle \quad (12)$$

form an orthonormal basis set and hence can serve as effective single particle orbitals with momentum \mathbf{k} . Since

the Boson operators which correspond to the original triplets obey [19] $[\tilde{\tau}_{\mathbf{k},\alpha}, \tilde{\tau}_{\mathbf{k},\beta}^\dagger] = N_{\alpha,\beta}$, the operators $\tau_{\mathbf{k},\nu}$ obey the canonical commutation relations for Boson operators: $[\tau_{\mathbf{k},\nu}, \tau_{\mathbf{k},\nu'}^\dagger] = \delta_{\nu,\nu'}$. They describe a triplet-like excitation which oscillates between x and y -directed bonds within a certain spatial region whose extent is determined by the range of the real space overlap integrals $\langle i, \alpha | j, \alpha' \rangle$.

Next, we set up the 2×2 Hamilton matrix $H(\mathbf{k}) = \langle \tau_{\mathbf{k},\nu} | H | \tau_{\mathbf{k},\nu'}^\dagger \rangle$, which in turn requires knowledge of the real space matrix elements $\langle i, \alpha | H | j, \alpha' \rangle$. Diagonalizing $H(\mathbf{k}) - E_0 N(\mathbf{k})$, where E_0 denotes the expectation value of H in the ‘background’ state (4), we obtain the desired dispersion relation of a single triplet Boson. The pair creation matrix element is obtained in an analogous way.

This procedure in fact is neither new nor unconventional: a completely analogous construction is performed e.g. in the construction of the $t - J$ model [20], which describes the dynamics of the (non-orthogonal) Zhang-Rice singlets on the different plaquettes of the CuO₂ plane. The only difference is that here we have two different nonorthogonal objects (Bosons on bonds in x and y -direction) per unit cell, whereas it was only a single Zhang-Rice singlet/unit cell in the case of the CuO₂ plane. Apart from that the construction is precisely the same.

In the next three sections we will calculate the dispersion relation, the pair creation matrix element, and discuss how these matrix elements depend on the density of triplets. Readers which are not interested in these more technical parts are advised to proceed to section VI.

III. PROPAGATION OF A SINGLE TRIPLET

To carry out our program we need to compute the real-space matrix elements $\langle i, \alpha | j, \beta \rangle$ and $\langle i, \alpha | H | j, \beta \rangle$. In doing so the concept of a loop covering of the plane [2] is of crucial importance. For two dimer coverings a and b the loop covering $c = a + b$ is obtained by drawing a and b ‘on top of each other’ (see for example Figure 1 in Ref. [2]). This produces a covering of the plane by closed loops u , each of even length $2L(u)$ (note that in the following we always measure the length of a loop $L(u)$ ‘in units of dimers’). Let us now consider each loop u as an isolated 1D ring with $2L(u)$ sites. We assume that the sites along the ring are labeled such that the dimer covering a corresponds to the state $|a\rangle = \prod_i s_{i,i+1}^\dagger |0\rangle$ - the dimer covering b then must correspond to $|b\rangle = \prod_i s_{i+1,i+2}^\dagger |0\rangle$. Expanding the products we get $2^{L(u)}$ different spin states from each covering, and there are precisely 2 spin states which show up in both $|a\rangle$ and $|b\rangle$ namely the two possible Néel states. We thus have $\langle a | b \rangle = 2/2^{L(u)}$. The same holds true for any other loop, whence, using $\sum_{u \in a+b} L(u) = N$, we find the scalar product of the two singlet distributions

[2]

$$\langle \psi_a | \psi_b \rangle = 2^{P(a+b)-N},$$

where $P(c)$ is the total number of loops in the loop covering c .

Let us now assume that the singlets on the bond m in $|\psi_a\rangle$ and on the bond n in $|\psi_b\rangle$ have been replaced by a z -like triplet (due to the explicit rotational invariance of the ‘singlet soup’ the result for an x -like or y -like Boson will be precisely the same - we are choosing the z -like component because the ambiguous states in this case are again the ones with Néel order along the loop). Then, a necessary condition for the scalar product to be different from zero is that there is a single loop u_0 in the resulting loop covering $a + b$ which passes through both bonds m and n . The reason is that the time-reversal parity of the triplet is negative whereas that of the singlet is positive. A necessary condition for a loop u to give a nonvanishing overlap is that the total time-reversal parities ‘along the loop’ are equal for both states $|\psi_a\rangle$ and $|\psi_b\rangle$. This, however, is only possible if the triplets in $|\psi_a\rangle$ and $|\psi_b\rangle$ are within the same loop. Each loop in $a + b$ therefore must contain either no triplet or both of them.

We can now split up the entire overlap integral $\langle \psi_a | \psi_b \rangle$ into components which differ by the length and topology of the loop u_0 which passes through both triplets. The absolute numerical value of the overlap from this particular loop is identical to the case of pure singlet covering. The only change may be an extra minus sign, which originates because the singlets do have an orientation, whereas the triplets do not. We thus can rewrite the overlap as

$$\langle \psi_a | \psi_b \rangle = \sum_{u_0} 2^{1-L(u_0)} (-1)^{\sigma(u_0)} \chi(u_0),$$

$$\chi(u) = \frac{2^{-(N-L(u))}}{n_1} \sum_{a,b} 2^{P(a+b)-1} \Delta_{a+b,u}. \quad (13)$$

Here $\Delta_{c,u}$ is 1 if the loop covering c contains the loop u and zero otherwise. We also note that $\chi(1)=1$, which fixes the normalization factor n_1 . With the exception of the $\chi(u)$ all parts in (13) can be computed analytically. $\chi(u)$ may be viewed as the norm of a nearest-neighbor RVB state which covers only the exterior of the loop u , divided by the norm n_1 of the state which covers the exterior of a single bond. If we assume that the norm increases exponentially with the number of sites in the system, $n \approx e^{\alpha N}$, with $\alpha > 0$, one would estimate that $\chi(u) \approx e^{-\alpha(L(u)-1)}$. This suggests that $\chi(u)$ is a quite rapidly decreasing function of $L(u)$. In the present work numerical values for $\chi(u)$ were obtained by exact calculations on finite clusters (see the Appendix). The $\chi(u)$ thereby indeed turned out to decay rapidly with $L(u)$, so only contributions with $L(u) \leq 2$ were kept in the present calculation. It should be noted that the computation of the $\chi(u)$ is no fundamental obstacle to the present

scheme: it may well be possible to obtain essentially exact values for these parameters by using Monte-Carlo techniques on large lattices. Figure 4 then shows the

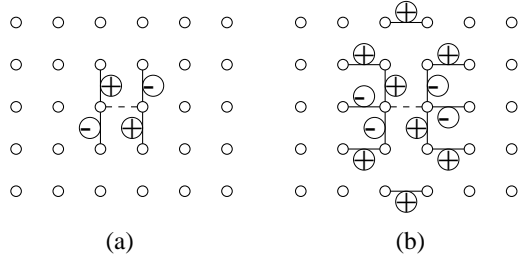


FIG. 4. Pairs of bonds which are connected by $L=2$ loops (a) and $L=3$ loops (b). Bond i is kept fixed (dashed line), bond j (full line) is labeled by $(-1)^{\sigma(u)}$.

pairs of bonds (i, α) and (j, β) which can be connected by loops of length 2 and 3 as well as the corresponding signs $(-1)^{\sigma(u_0)}$. In this way we find the overlap matrix

$$N(\mathbf{k}) = \sum_{L=1}^{\infty} \frac{\chi(L)}{2^{L-1}} \gamma_L(\mathbf{k})$$

with $\gamma_1(\mathbf{k})=1$ and

$$\gamma_2(\mathbf{k}) = \begin{pmatrix} 0 & 4 \sin(\frac{k_x}{2}) \sin(\frac{k_y}{2}) \\ 4 \sin(\frac{k_x}{2}) \sin(\frac{k_y}{2}) & 0 \end{pmatrix}. \quad (14)$$

We proceed to a calculation of the matrix elements of the Hamiltonian. We first recall that for the nearest neighbor RVB state the expectation value of H between two dimer coverings $|\psi_a\rangle$ and $|\psi_b\rangle$ can be decomposed into contributions from each individual loop in the loop covering $a+b$ [2]:

$$\langle \psi_a | H | \psi_b \rangle = [\sum_{u \in a+b} E(u)] 2^{P(a+b)-N},$$

$$E(u) = \epsilon_s [(2 - \delta_{L(u),1}) L(u) + n_b(u)],$$

where $n_b(u)$ is the number of nearest-neighbor bonds in u which bridge the loop (see Figure 5), and $\epsilon_s = -3J/4$ the exchange energy/singlet. $E(u)/\epsilon_s$ is the number of nearest-neighbor bonds that can be formed from the sites covered by u [2]. This formula implies that there is no

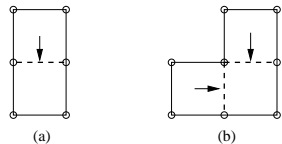


FIG. 5. ‘Bridging bonds’ (dashed lines) in the $L = 3$ loop (a) and in an $L = 4$ loop (b).

contribution from bonds connecting *different loops*. The reason is that the exchange along a bond connecting different singlets can only lead to the pair creation of two triplets, see the first equation (7). In order to maintain time reversal symmetry along each loop, it is then necessary that both triplets belong to the same loop - which is not possible if the bond in question connects different loops.

Let us now again assume that the bond m in $|\psi_a\rangle$ and the bond n in $|\psi_b\rangle$ are occupied by a triplet, and consider the ‘connected matrix element’ of H between the two resulting states: $\langle \psi_b | H | \psi_a \rangle - E_0 \langle \psi_b | \psi_a \rangle$. First, let us assume that we act with the exchange along a bond connecting m and a neighboring bond m' ; the triplet can either propagate from m to m' , or decay into two triplets on both m and m' (see the second Equation (7)). Neglecting the second possibility we obtain a nonvanishing contribution to the matrix element of H only if there is a single loop $u_0 \in a+b$ which covers both, m' and n . Alternatively, if we act on a bond which connects n and a neighboring bond n' , the triplet jumps from n to n' and we get a nonvanishing contribution only if one single loop $u_0 \in a+b$ covers n' and m . If, on the other hand, we act with the exchange along a bond which does not touch either of the triplet bonds m or n , both triplets will stay where they are and we get a nonvanishing matrix element only if both, m and n , are covered by a single loop $u_0 \in a+b$. The same holds true if we act with the exchange along the bonds m and n themselves.

We first consider the case that m and n belong to two different loops, u_0 and u'_0 . In the simplest case both ‘loops’ consist only of a single bond, i.e. u_0 consists of the single bond m and u'_0 only of n . Since the two triplets belong to different loops, the overlap $\langle \psi_b | \psi_a \rangle$ is zero. Moreover, the matrix elements of the exchange along any bond which does not connect m and n vanishes - the calculation thus becomes very easy. The matrix element for the triplet hopping from m to n is $\pm J/4$, where the signs for different relative positions of the two bonds are shown in Figure 6. To ‘embed’ the hopping process

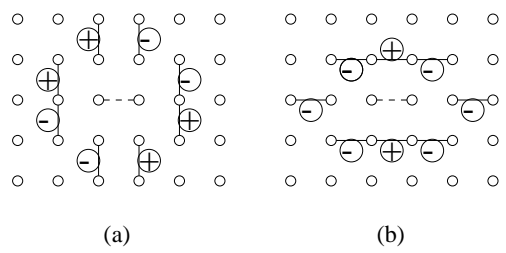


FIG. 6. The sign of the hopping integral from the dashed bond m (dashed) to the indicated bond n .

into the singlet background, we need to renormalize this matrix element by

$$\eta_{nm} = \frac{2^{-N}}{n_1} \sum_{a,b} 2^{P(a+b)} \Delta_{a+b,m} \Delta_{a+b,n}, \quad (15)$$

which is again estimated from cluster calculations. The first contribution to the Hamilton matrix then is:

$$\epsilon^{(1)}(\mathbf{k}) = \frac{J\eta}{4} t_1(\mathbf{k}), \quad (16)$$

where the elements of the 2×2 matrix $t_1(\mathbf{k})$ are:

$$\begin{aligned} t_{1,xx}(\mathbf{k}) &= 4 \cos(k_y) - 2 \cos(2k_x) - 4 \cos(k_x) \cos(k_y), \\ t_{1,yy}(\mathbf{k}) &= 4 \cos(k_x) - 2 \cos(2k_y) - 4 \cos(k_x) \cos(k_y), \\ t_{1,xy}(\mathbf{k}) &= 4 \sin\left(\frac{3k_x}{2}\right) \sin\left(\frac{k_y}{2}\right) + 4 \sin\left(\frac{3k_y}{2}\right) \sin\left(\frac{k_x}{2}\right). \end{aligned} \quad (17)$$

To keep things simple we have moreover replaced the different η_{nm} by the average value η .

Next, we consider the case that one of the loops, e.g. u'_0 , has a length ≥ 2 . In other words, we are considering a process like the one shown in Figure 7: the triplet jumps from bond m to bond m' , and the triplet on m'

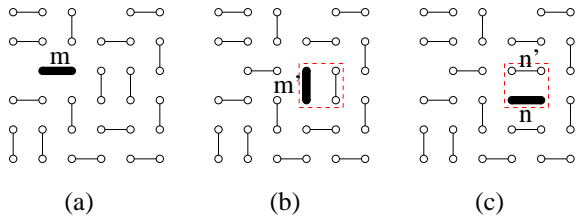


FIG. 7. By application of H a triplet can hop from bond $m \rightarrow m'$ (see (a) \rightarrow (b)) and then overlap with the triplet in the final state on bond n along the indicated $L = 2$ -loop (see (b) \rightarrow (c)). This process gives a nonvanishing hopping matrix element from bond $m \rightarrow n$.

overlaps with the triplet on bond n along a loop (in this case of length 2). There is also an analogous process, where the triplet jumps from n to m' and m' and m overlap by a loop. The respective matrix elements can be factorized into the matrix element for the hopping of the triplet times the overlap along the loop. This means that the matrix element can be written as $\frac{\eta_3 J}{8} t_2(m, n)$ where

$$t_2(m, n) = \sum_{m'} [t_1(m, m') \gamma_2(m', n) + t_1(n, m') \gamma_2(m', m)];$$

here $t_1(m, m')$ and $\gamma_2(m', n)$ are the real-space versions of the matrices (17) and (14). Fourier transformation gives

$$\epsilon^{(2)}(\mathbf{k}) = \frac{\eta_3 J}{8} (t_1(\mathbf{k}) \gamma_2(\mathbf{k}) + \gamma_2(\mathbf{k}) t_1(\mathbf{k})) \quad (18)$$

where it has to be kept in mind that $t_1(\mathbf{k})$ and $\gamma_2(\mathbf{k})$ are *symmetric* 2×2 matrices. The ‘embedding factor’ is

$$\eta_3 = \frac{2^{-N}}{n_1} \sum_{a,b} 2^{P(a+b)} \Delta_{a+b,m} \Delta_{a+b,n'} \Delta_{a+b,n} \quad (19)$$

where (m, n', n) are like in Figure 7. Actually there are two inequivalent relative orientations of a single bond m and an $L = 2$ loop - the two respective values of η_3 do not differ strongly and for simplicity we use the average of the two values for the two configurations. Processes involving even longer loops could be treated in an analogous way, but we neglect these.

We proceed to the second case, i.e. we assume that m and n are covered by a single loop u_0 . As was the case for the overlap integrals, the matrix elements then can be split up into contributions differing by the loop u_0 which covers both triplet bonds. Once this loop is fixed, we can divide all bonds in the plane into three distinct classes. First, bonds belonging to any loop other than u_0 are not affected at all by the presence of the triplets and give the same contribution as in the pure singlet state. This becomes

$$2^{1-L(u_0)} (-1)^{\sigma(u_0)} \frac{2^{-(N-L(u_0))}}{n_1} \sum_{a,b} \left[\sum_{\substack{u \in a+b \\ u \neq u_0}} E(u) \right] 2^{P(a+b)-1} \Delta_{a+b,u_0}. \quad (20)$$

This is an energy of order of the system size N ; in the end it must be canceled, up to terms of order N^0 , by a corresponding contribution in $-E_0 \langle \psi_a | \psi_b \rangle$. This cancellation is the analogue of the familiar linked-cluster theorem of many-body physics.

Second, we consider those bonds in u_0 which are not bridging bonds. They will be covered by either a singlet or a triplet in either a or b , whence these bonds together give the contribution

$$[E(u_0) + (2 - \delta_{L(u_0),1}) J - \epsilon_s n_b(u_0)] 2^{1-L(u_0)} (-1)^{\sigma(u_0)} \chi(u_0). \quad (21)$$

This is a ‘connected’ contribution of order N^0 .

This leaves us with the bridging bonds (see Figure 5), which may give a nontrivial contribution. However, since the bridging bonds occur only for $L(u_0) \geq 3$ we neglect their contribution altogether.

The subtracted contribution, $-E_0 \langle \psi_a | \psi_b \rangle$, may be rewritten as

$$-E_0 \sum_{u_0} 2^{1-L(u_0)} (-1)^{\sigma(u_0)} \frac{2^{-(N-L(u_0))}}{n_1} \sum_{a,b} 2^{P(a+b)-1} \Delta_{a+b,u_0}, \quad (22)$$

where we have used the expanded form (13) of $\chi(u_0)$. This is again an energy of order N , which cancels the bulk term (20) up to terms of order N^0 . After some reshuffling (using $\sum L(u)=N$) we can rewrite the contribution to the matrix element as

$$J\langle\psi_a|\psi_b\rangle + \sum_{u_0} (\epsilon_J(u_0) + \epsilon_0(u_0)) \quad (23)$$

with

$$\begin{aligned} \epsilon_J(u) &= J (1 - \delta_{L(u_0),1}) 2^{1-L(u)} (-1)^{\sigma(u)} \chi(u) \\ \epsilon_0(u) &= \frac{(-1)^{\sigma(u)}}{n_1} \sum_{a,b} \left[\sum_{u \in a+b} \bar{E}(u) \right] 2^{P(a+b)-N} \Delta_{a+b,u} \\ \bar{E}(u) &= E(u) - L(u) \frac{E_0}{N}. \end{aligned} \quad (24)$$

The first term on the rhs of (23) is the ‘bare’ on-site energy of the triplet. It is always proportional to the overlap integral, so upon switching to the effective Bosons this term becomes a \mathbf{k} -independent constant shift. The quantity $\epsilon_0(u)$ may be thought of as describing a ‘loss of resonance energy’. It is the difference of the two contributions (20) and (22) and occurs because the loop u_0 is fixed, whence the area covered by this loop is not available for resonating between different singlet coverings. For example we have

$$J + \epsilon_0(1) = \frac{\langle\psi_a|H|\psi_a\rangle}{\langle\psi_a|\psi_a\rangle} - E_0, \quad (25)$$

i.e. this quantity is an additive renormalization of the energy of formation for a single triplet due to its being ‘embedded into the singlet soup’. Numerical evaluation in a cluster shows that this additive correction is quite large - for one triplet in a pure singlet background we find $\epsilon_0(1) \approx 1.2J$. While this is surprising at first sight it should be noted that a similar large value ($\approx 0.8J$) was previously found in spin ladders [9]. A fixed triplet obviously leads to a quite substantial loss of resonance energy. The numerical values of $\epsilon_0(u)$ and E_0 were again obtained by cluster calculations (Appendix). Introducing $\tilde{\epsilon}_0(u)=\epsilon_0(u)+J\chi(u)$ we can write down the third part of the Hamilton matrix:

$$\tilde{\epsilon}^{(3)}(\mathbf{k}) = \epsilon_0(1) + \sum_{L \geq 2} \frac{\tilde{\epsilon}_0(L)}{2^{L-1}} \gamma_L(\mathbf{k}) \quad (26)$$

We can now add up the three contributions, (16), (18), and (26) to obtain the total ‘connected’ Hamilton matrix $\tilde{\epsilon}(\mathbf{k})$. This is still expressed in terms of the non-orthogonal orbitals $\tilde{\tau}_{\mathbf{k},\alpha}^\dagger$. What remains to be done therefore is to transform the Hamilton matrix to the orthogonal orbitals (12). To that end we take matrix elements of the form $\langle\nu, \mathbf{k}|\tilde{\epsilon}(\mathbf{k})|\nu', \mathbf{k}\rangle$. Introducing the 2×2 transformation matrix

$$T = \left(\frac{1}{\sqrt{\lambda_1}} \mathbf{e}_1, \frac{1}{\sqrt{\lambda_2}} \mathbf{e}_2 \right), \quad (27)$$

the transformed Hamiltonian then can be expressed as

$$\epsilon(\mathbf{k}) = T^T \tilde{\epsilon}(\mathbf{k}) T.$$

IV. PAIR CREATION AMPLITUDE

In this section we proceed to a discussion of the pair creation amplitude $\Delta_{\mathbf{k}}$ in equation (9). As discussed in section II, by starting from an arbitrary singlet covering of the plane and acting with the Hamiltonian along a bond connecting two different singlets, we *only* create a state where both singlets are replaced by triplets, see the first of Eqs. (7). The situation where the two singlets in question are ‘parallel’ to each other, i.e. that the 4 sites belonging to the 2 singlets form a square with edge 1, requires special attention. As discussed above we have the identity

$$s_{i,j}^\dagger s_{i',j'}^\dagger |0\rangle - 2s_{i,i'}^\dagger s_{j,j'}^\dagger |0\rangle = \mathbf{t}_{i,j}^\dagger \cdot \mathbf{t}_{i',j'}^\dagger |0\rangle, \quad (28)$$

i.e. the state with two parallel triplets can be expressed as a linear combination of the two perpendicular combinations of parallel singlet states. In other words: this state is already exhausted by the singlet background, and consequently must be omitted from our reduced Hilbert space. The triplets thus have to obey the additional constraint of never being parallel to each other - one implication is that we must set the respective pair creation matrix element to zero.

To compute the numerical value of the matrix element, let us consider the action of H on the RVB state (3). We have

$$\begin{aligned} H|RVB\rangle &= N\epsilon_s|RVB\rangle \\ &+ \frac{J(-1)^{\sigma(m,n)}}{4} \frac{n_1}{\sqrt{n}} \sum_{m,n} \sum'_{\alpha} |\Phi_{m\alpha,n\alpha}\rangle. \end{aligned} \quad (29)$$

The first term on the rhs originates from processes where the Hamiltonian has ‘hit’ a bond covered by a singlet, the second one originates from processes where the exchange has acted along bonds connecting two singlets on bonds m and n (the prime on the sum indicates that only pairs of bonds connected by a bond are summed over). The modulus of the respective matrix element is $J/4$ (see equation (7)) and there is an extra sign which depends on the relative orientation of the bonds m and n . The dependence of this sign on the orientation is shown in Figure 8. Also, we have approximated the normalization factor which is included in the definition of $|\Phi_{m\alpha,n\alpha}\rangle$ by

$$\frac{1}{n(m\alpha, n\alpha)} \approx \frac{1}{\sqrt{n_1^2}}. \quad (30)$$

The factor of $1/\sqrt{n}$ remains from the definition of (3). To obtain the pair creation matrix element we now form the overlap between (29) and the state $\tau_{\mathbf{k},\nu}^\dagger \tau_{-\mathbf{k},\mu}^\dagger |0\rangle$.

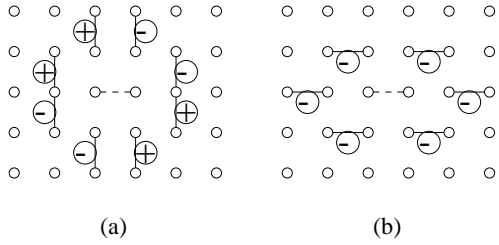


FIG. 8. The sign $(-1)^{\sigma(m,n)}$ for all different pairs of bonds on which pair creation is possible. The bond m (dashed) is kept fixed, the bond n is labeled by $(-1)^{\sigma(m,n)}$.

Defining the 2×2 matrix

$$\tilde{\Delta}(\mathbf{k}) = \frac{\zeta J}{8} t'_{1,\alpha\beta}(\mathbf{k}),$$

$$\zeta = \frac{n_1}{\sqrt{n}},$$

$$\begin{aligned} t'_{1,xx}(\mathbf{k}) &= -2 \cos(2k_x) - 4 \cos(k_x) \cos(k_y), \\ t'_{1,yy}(\mathbf{k}) &= -2 \cos(2k_y) - 4 \cos(k_x) \cos(k_y), \\ t'_{1,xy}(\mathbf{k}) &= 4 \sin\left(\frac{3k_x}{2}\right) \sin\left(\frac{k_y}{2}\right) + 4 \sin\left(\frac{3k_y}{2}\right) \sin\left(\frac{k_x}{2}\right), \end{aligned} \quad (31)$$

and bearing in mind that $\langle \bar{\tau}_{\mathbf{k},\alpha} | \bar{\tau}_{\mathbf{k},\alpha'}^\dagger \rangle = N_{\alpha,\alpha'}(\mathbf{k})$, we find for the pair creation matrix:

$$\Delta(\mathbf{k}) = T^T N(\mathbf{k}) \tilde{\Delta}(\mathbf{k}) N^T(\mathbf{k}) T.$$

This completes the derivation of the single-particle terms of the triplet Hamiltonian. Before we proceed, let us briefly return to the problem of non-orthogonality. Strictly speaking, the state with two triplets is not orthogonal to the singlet background either. The reason is that if one draws a loop passing through both triplets, the time reversal parities of the two triplets cancel, and the state has a nonvanishing overlap with a state where the loop is covered only by singlets (see Figure 9).

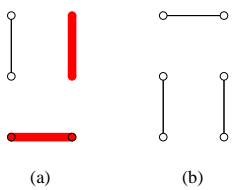


FIG. 9. A state with two triplets (a) can have a nonvanishing overlap with a state consisting exclusively of two singlets (b).

However, this overlap is rather small: in the case shown in Figure (9) it is for example $-\sqrt{3}\chi(3)/8$, and obviously this is the most unfavorable case. For other relative orientations of the two triplets the overlap can be only achieved by a loop of length 8, whence these overlaps are $\propto \chi(4) \ll 1$. The non-orthogonalities thus are much more benign than those for the spinon-states, whence neglecting them altogether (as we will do henceforth) is probably quite justified.

V. EXTRAPOLATION TO FINITE TRIPLET DENSITY

In the preceding sections we have computed the various overlap integrals and matrix elements for triplet propagation, pair creation and interaction. In all of these cases the matrix element could be factorized into a contribution from a ‘local’ transition between different singlet/triplet coverings along a single or two neighboring loops, and a factor which describes the embedding of these active loops into the singlet background. Thereby we have always given expressions for these ‘embedding factors’ which are valid in the limit of vanishing triplet concentration, i.e. we have computed them as they would be for a pure singlet covering of the system. Clearly, this is inappropriate for the real system, where quantum fluctuations have admixed a finite density of triplet Bosons. In the following we want to discuss how we have to modify our theory to take the effect of a finite triplet concentration into account. It should be stressed from the very beginning that this is quite obviously a very complex problem and we will be forced to apply some relatively crude approximations.

If we want to derive single-particle like matrix elements for finite triplet concentration we should consider overlap integrals or matrix elements of H of the type

$$\langle \Psi_{i_1 \alpha_1, i_2 \alpha_2, \dots, i_m \alpha_m} | \Psi_{i_1 \alpha_1, i_2 \alpha_2, \dots, i_m \alpha_m} \rangle, \quad (32)$$

i.e. $m-1$ triplets stay unchanged, and only a single one (which without loss of generality can be taken to be the first one) changes its position (but maintains its spin). In other words, we should calculate the embedding factors for singlet coverings containing a certain number of ‘inert’ triplets. Thereby we actually have to make the major *assumption* that the matrix element does not depend significantly on the positions of these inert triplets - otherwise, the very idea of a single particle-like propagation of the triplets would be invalid. One might then expect that approximate values can be obtained by distributing the m inert triplets in all possible ways (we call the number of possible distributions $D(m)$) over the system, and taking the average of the respective matrix elements computed for all $D(m)$ possible distributions. In this way, the embedding factors acquire a dependence

on the density of triplets.

The numerical calculation in a finite cluster then proceeds as follows: we choose m bonds $i_1, i_2 \dots i_m$, which obey the various constraints on the relative positions of triplets, and evaluate the ground state norm and energy according to

$$n = \sum_{a,b} 2^{P(a+b)-N} \prod_{\nu=1}^m \Delta_{a+b,i_\nu},$$

$$E_0 = \sum_{a,b} \left[\sum_{u \in a+b} \epsilon(u) \right] 2^{P(a+b)-N} \prod_{\nu=1}^m \Delta_{a+b,i_\nu}. \quad (33)$$

The calculation of the various embedding factors then proceeds in an entirely analogous fashion i.e. in (13), (15), and (24) we replace

$$\sum_{a,b} \dots \rightarrow \sum_{a,b} \left(\prod_{\nu=1}^m \Delta_{a+b,i_\nu} \right) \dots \quad (34)$$

In this way we obtain all embedding factors for fixed distribution of inert triplets, and the value for triplet concentration m/N is obtained by averaging over all allowed distributions of the bonds $i_1, i_2 \dots i_m$. In practice this calculation requires quite a substantial numerical effort so this was performed only for the 4×4 cluster.

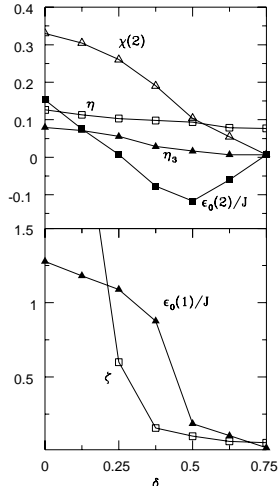


FIG. 10. Dependence of the various parameters on the triplet density δ as obtained from numerical calculations on the 4×4 cluster.

One might expect, however, that the finite size effects are in fact smaller for the more relevant higher triplet concentrations: the main effect of the fixed triplets obviously is to reduce the importance of long loops. Since the bonds occupied by the static triplets must be identical in the bra and ket state, loops of length $L(u) \geq 2$ which pass through these bonds are impossible. When the density of triplets gets appreciable, the probability to find enough space for forming longer loops becomes

smaller and smaller. Since longer loops may cause problems in the small clusters, a suppression of these may therefore even reduce finite-size effects. Moreover, the suppression of longer loops is actually beneficial for our entire approach: it tends to eliminate the problems with the nonorthogonalities in the singlet soup and makes the truncation of the length $L(u_0)$ a better approximation.

As an illustration Figure 10 shows the dependence of $\epsilon_0(1)$, i.e. the additive renormalization of the energy of formation of a triplet (see (25), evaluated in the 4×4 cluster. The concentration dependence is as expected: for low triplet concentration $\epsilon_0(1)$ is large because an added triplet blocks many long loops along which resonance could have occurred. As the triplet concentration gets higher, these longer loops are blocked anyway, so adding a further triplet does not increase the energy too much any more. In the high-density limit the additive renormalization approaches zero, as expected. The Figure shows, however, that the concentration dependence is quite significant, i.e. this effect should not be neglected.

In addition to reducing the importance of longer loops, for a finite density of triplets we have to take care of the excluded volume constraint which the bond Bosons have to obey. Placing a triplet on one given bond m blocks a total of 9 other bonds, on which no more triplets can be placed (see Figure 11).

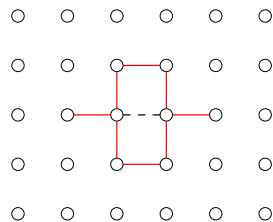


FIG. 11. Placing a triplet on the central (dashed) bond blocks the 9 indicated bonds, on which no more triplet can be placed.

Of these, 7 bonds are blocked because they share a site with m , the remaining 2 are blocked because they are ‘parallel’ to m and the state with two parallel triplets is actually a linear combination of singlets (see (28)). In order to take care of this *blocking effect*, we resort to a Gutzwiller-type approximation. It has been shown by Ogawa *et al.* [21] that the essence of the Gutzwiller approximation is the neglect of the difference in phase between states where the particles in question are distributed in different ways over the lattice. With this approximation, any real space distribution of m Bosons contributes the same number (which without loss of generality can be taken to be 1) to the norm of any state with m Bosons. The total norm of any such state then becomes simply the number of possible ways to distribute m Bosons over the plane, i.e. $D(m)$. In the present case,

the situation is somewhat more complicated, because we still have to take into account the fact that due to the loop problem the norm of a state with m fixed triplets is not 1 (unlike the case if the triplets were just ordinary Bosons). We thus approximate the normalization factor of any state with m triplets by

$$n(m) = \frac{1}{\sqrt{D(m)n_m^-}}, \quad (35)$$

where n_m^- is the value obtained by averaging (33) over all allowed triplet configurations $i_1, i_2 \dots i_m$. Clearly, this replacement will lead to a renormalization of the various embedding factors. To evaluate these, we usually have to consider a certain area \mathcal{A} , covered by one or two loops, in which the actual overlap, hopping or pair creation process takes place. We then determine (again by simulation on the 4×4 cluster) the number of ways to distribute m triplets over the exterior of the area \mathcal{A} . Thereby we request that putting a triplet anywhere within \mathcal{A} always gives an allowed configuration of $m+1$ triplets. We call the number of allowed triplet configurations $D(m, \mathcal{A})$. Defining the various areas \mathcal{A}_i as

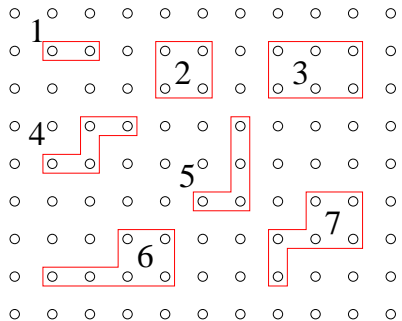


FIG. 12. Areas on which no triplets are allowed in some processes.

in figure 12, we then have to renormalize the various parameters as follows:

$$\begin{aligned} n_1 &\rightarrow \frac{n_1}{\sqrt{D(m, \mathcal{A}_1)}}, \\ \chi(2) &\rightarrow \chi(2) \frac{D(m, \mathcal{A}_2)}{D(m, \mathcal{A}_1)}, \\ \epsilon_0(2) &\rightarrow \epsilon_0(2) \frac{D(m, \mathcal{A}_2)}{D(m, \mathcal{A}_1)}, \\ \eta &\rightarrow \eta \frac{D(m, \mathcal{A}_4) + D(m, \mathcal{A}_5)}{2D(m, \mathcal{A}_1)}, \\ \eta_3 &\rightarrow \eta_3 \frac{D(m, \mathcal{A}_6) + D(m, \mathcal{A}_7)}{2D(m, \mathcal{A}_1)}. \end{aligned} \quad (36)$$

For the pair creation amplitude we replace

$$\zeta \rightarrow \frac{\zeta}{2} \left(\sqrt{\frac{D(m, \mathcal{A}_4)}{n}} + \sqrt{\frac{D(m, \mathcal{A}_5)}{n}} \right) \quad (37)$$

To summarize this section, Figure 10 shows the values of the different parameters as estimated by the procedure outlined above, for all possible triplet concentrations in the 4×4 cluster. Let us stress again that the approximations leading to the parameters in Figure 10 are probably rather crude - one may expect, however that we get roughly correct orders of magnitude and that the ratios of the different parameters come out approximately correct.

VI. SPIN DYNAMICS

Let us first briefly summarize the discussion so far: We have shown that the elementary excitations of the singlet soup correspond to excited dimers, which must be modeled by bond-Bosons. Combining the matrix elements computed in the two preceding sections we obtain a Hamiltonian of the form

$$H = \sum_{\mathbf{k}, \nu, \mu} \epsilon(\mathbf{k})_{\nu, \mu} \boldsymbol{\tau}_{\mathbf{k}, \nu}^\dagger \cdot \boldsymbol{\tau}_{\mathbf{k}, \mu} + (\Delta(\mathbf{k})_{\nu, \mu} \boldsymbol{\tau}_{\mathbf{k}, \nu}^\dagger \cdot \boldsymbol{\tau}_{-\mathbf{k}, \mu}^\dagger + H.c.).$$

Thereby the matrix elements $\Delta(\mathbf{k})$ and $\epsilon(\mathbf{k})$ are functions of the triplet density. For given triplet density δ_i these parameters can be computed and the Hamiltonian, which after the Gutzwiller-type renormalization of the matrix elements we take to be a free-Boson Hamiltonian, is solved by Bogoliubov transformation. Combining the two different τ -operators into a 2-vector \mathbf{T} the ansatz reads

$$\mathbf{T}_{\mathbf{k}} = u_{\mathbf{k}} \mathbf{T}_{\mathbf{k}} + v_{\mathbf{k}} \mathbf{T}_{-\mathbf{k}}^\dagger, \quad (38)$$

where the real 2×2 matrices u and v have to fulfill

$$\begin{aligned} u_{\mathbf{k}} u_{\mathbf{k}}^T - v_{\mathbf{k}} v_{\mathbf{k}}^T &= 1, \\ u_{\mathbf{k}} v_{\mathbf{k}}^T - v_{\mathbf{k}} u_{\mathbf{k}}^T &= 0. \end{aligned} \quad (39)$$

The inverse transformation of (38) is therefore

$$\mathbf{T}_{\mathbf{k}} = u_{\mathbf{k}}^T \mathbf{\Gamma}_{\mathbf{k}} - v_{\mathbf{k}}^T \mathbf{\Gamma}_{-\mathbf{k}}^\dagger, \quad (40)$$

The Hamiltonian can be transformed to free particle form:

$$\begin{aligned} H &= \sum_{\mathbf{k}, \nu} \omega_{\nu}(\mathbf{k}) \mathbf{\Gamma}_{\mathbf{k}, \nu}^\dagger \mathbf{\Gamma}_{\mathbf{k}, \nu} + \\ &+ 3 \sum_{\mathbf{k}} \text{Tr}[v_{\mathbf{k}} \epsilon(\mathbf{k}) v_{\mathbf{k}}^T - v_{\mathbf{k}} \Delta(\mathbf{k}) u_{\mathbf{k}}^T - u_{\mathbf{k}} \Delta(\mathbf{k}) v_{\mathbf{k}}^T], \end{aligned} \quad (41)$$

provided the transformation matrices obey

$$\begin{aligned} \epsilon(\mathbf{k}) u_{\mathbf{k}}^T - 2\Delta(\mathbf{k}) v_{\mathbf{k}}^T &= u_{\mathbf{k}}^T \omega(\mathbf{k}), \\ 2\Delta(\mathbf{k}) u_{\mathbf{k}}^T - \epsilon(\mathbf{k}) v_{\mathbf{k}}^T &= v_{\mathbf{k}}^T \omega(\mathbf{k}). \end{aligned} \quad (42)$$

Here we have introduced the 2×2 matrix $\omega(\mathbf{k}) = \text{diag}(\omega_1(\mathbf{k}), \omega_2(\mathbf{k}))$. The triplet density is

$$\delta_f = \frac{3}{N} \sum_{\mathbf{k}} \text{Tr}[u_{\mathbf{k}} u_{\mathbf{k}}^T f(\omega) + v_{\mathbf{k}} v_{\mathbf{k}}^T (1 + f(\omega))], \quad (43)$$

where f is the Bose function. The requirement $\delta_i = \delta_f$ then provides a self-consistency condition for the density. Numerical evaluation shows that there is a minimum triplet concentration δ_0 . For $\delta < \delta_0$, the parameters are such that in a certain area around $\mathbf{k} = (\pi, \pi)$ the eigenvalue problem (42) does not have real eigenvalues. For δ_0 the minimum of the triplet dispersion, which occurs at (π, π) is precisely zero. With the coarse mesh of concentrations possible in the 16-site cluster, we find $0.25 < \delta_0 < 0.375$. We therefore linearize all matrix elements x , i.e. $x(\delta) = a_x + b_x(\delta - 0.25)$, using the values at $\delta = 0.25$ and $\delta = 0.375$ to determine a_x and b_x . This gives $\delta_0 = 0.335$.

With increasing temperature, the self-consistent value of δ increases slowly, approaching δ_0 for $T \rightarrow 0$. Figure 13 shows the dispersion relation for the respective self-consistently determined triplet density at different temperatures. Since we have two degrees of freedom/site (the triplet in x and y direction) we obtain two bands. While one of these bands is practically dispersionless, the dispersive one resembles results obtained for other spin

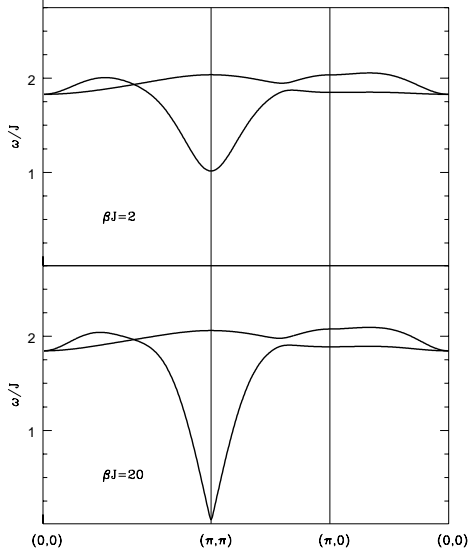


FIG. 13. Dispersion of the two eigenvalues ω_i , for two different temperatures.

liquids, such as the two-leg ladder [8,9] or the bi-layer Heisenberg antiferromagnet [11]: the dispersion starts at relatively high energy at $\mathbf{k} = (0, 0)$, takes a shallow maximum near the antiferromagnetic zone boundary and, as stated above, takes a more or less pronounced minimum at $\mathbf{Q} = (\pi, \pi)$. For low temperatures the bandwidth is $\approx 2J$, which is quite close to the value for antiferromag-

netic spin waves. The case of zero temperature requires special attention: it is obvious from Figure 13 that the gap at \mathbf{Q} approaches zero for $T \rightarrow 0$. Assuming that the gap vanishes at zero temperature, we may then assume that this momentum becomes macroscopically occupied by a triplet density $\delta_{\mathbf{Q}}$. To determine this condensed fraction we note that the limiting density δ_0 is defined such that the gap at \mathbf{Q} is exactly zero with the parameters calculated for this density. Then, for $\delta_i = \delta_0$ we evaluate the density $\bar{\delta}_f$ of uncondensed triplets (i.e. we exclude $\mathbf{k} = \mathbf{Q}$ from the sum in (43)) and finally determine the condensate density from

$$\delta_{\mathbf{Q}} = \delta_0 - \bar{\delta}_f. \quad (44)$$

This is entirely analogous to the treatment of Hirsch and Tang [22] of the condensation of Schwinger-Bosons in the mean-field theory of Arovas and Auerbach [23]. As will be seen in a moment, just as for the Schwinger Bosons the condensation of the triplets corresponds to antiferromagnetic ordering. The ground state energy then is

$$E_{\text{tot}} = E_0(\delta) - 3 \sum_{\mathbf{k}} \text{Tr}[v_{\mathbf{k}} v_{\mathbf{k}}^T \omega(\mathbf{k})] \quad (45)$$

where $E_0(\delta)$ is the energy of the singlet background for triplet density δ . This is calculated from (33). We obtain a value of $-0.3426J/\text{bond}$, which is quite close to the true ground state energy of the 2D Heisenberg antiferromagnet [24]. An interesting figure is the lowering of the energy as compared to the original RVB-vacuum (3). In the 4×4 cluster (which has been used to compute all matrix elements) the expectation value of the pure nearest-neighbor RVB state is $-0.334318J/\text{bond}$ [3], so that the admixture of the triplets lowers the energy only by a tiny $0.008J/\text{bond}$. In view of the strong approximations we were forced to make this result probably has little quantitative significance - it shows quite clearly, however, that the energy of the RVB-vacuum is lowered only by a very small energy by the triplet fluctuations. This is what must come out because in the thermodynamic limit the energy of the RVB state is $-0.302J/\text{bond}$ [16], compared to the exact ground state energy of approximately $0.334J/\text{bond}$ [24].

We proceed to a discussion of the spin correlation function. Since the bond-Bosons are actually objects which extend over more than one unit-cell, they have something like a structure factor which depends on the type of operator by which they are probed. Let us consider a single bond, (i, j) , and introduce even and odd combinations of spin operators on this bond:

$$S_{\pm}^z = S_i^z \pm S_j^z.$$

Due to their opposite parity under exchange of i and j these two operators have an entirely different effect on the 4 possible spin states of the bond: S_{\pm}^z annihilates

the singlet and t_z^\dagger but converts $t_x^\dagger \rightarrow it_y$ and $t_y^\dagger \rightarrow -it_x$, whence $S_+^z = i\bar{\tau}^\dagger \times \bar{\tau}$. S_-^z on the other hand converts the singlet into t_z^\dagger and vice versa, but annihilates both t_x^\dagger and S_+^z , whence $S_-^z = \bar{\tau}^\dagger + \bar{\tau}$. If we still restrict ourselves to only a single bond n we have to ‘translate’

$$\sum_j e^{i\mathbf{q} \cdot \mathbf{R}_j} \mathbf{S}_j = i \sum_n e^{i\mathbf{q} \cdot \mathbf{R}_n} [\cos\left(\frac{\mathbf{e}_n \cdot \mathbf{q}}{2}\right) \bar{\tau}_n^\dagger \times \bar{\tau}_n - \sin\left(\frac{\mathbf{e}_n \cdot \mathbf{q}}{2}\right) (\bar{\tau}_n^\dagger + \bar{\tau}_n)], \quad (46)$$

where \mathbf{q}_n is the unit vector along the bond n and \mathbf{R}_n denotes its center of gravity. Let us next discuss how these matrix elements are modified due to the embedding into the singlet background. We act with the operator $\mathbf{S}(\mathbf{q}) = (1/\sqrt{2N}) \sum_j e^{i\mathbf{q} \cdot \mathbf{R}_j} \mathbf{S}_j$ on some given state. The first term simply changes the z -spin and momentum of a triplet. It does not affect the number of triplets, so we need no further renormalizations. For the second term, let us start out from a state with one triplet, $|j, \alpha\rangle$, and assume that the triplet is annihilated, i.e. converted into a singlet. This leaves us with the state

$$|\psi_j\rangle = \frac{1}{\sqrt{n_1}} \frac{S^{N-1}}{(N-1)!} s_{j,j+\hat{\alpha}}^\dagger |0\rangle.$$

The matrix element with the pure RVB state then is

$$\langle RVB | \psi_j \rangle = \frac{1}{\sqrt{nn_1}} \frac{n}{4} = \frac{1}{4} \sqrt{\frac{n}{n_1}},$$

because it is easy to see that a state with one fixed singlet has an overlap of $n/4$ with the RVB state. If we want to extrapolate this to finite triplet density we again have to use the values of n and n_1 computed with m fixed triplets, and renormalize the matrix element by

$$\kappa = \sqrt{\frac{D(m, \mathcal{A}_1)}{D(m)}}.$$

We thus find

$$\begin{aligned} \mathbf{S}(\mathbf{q}) = & \sum_{\alpha=x,y} [\cos(\frac{q_\alpha}{2}) \frac{1}{\sqrt{2N}} \sum_{\mathbf{k}} \bar{\tau}_{\mathbf{q}+\mathbf{k},\alpha}^\dagger \times \bar{\tau}_{\mathbf{k},\alpha} \\ & - \frac{\kappa}{4} \sqrt{\frac{n}{n_1}} \sin(\frac{q_\alpha}{2}) (\bar{\tau}_{\mathbf{q},\alpha}^\dagger + \bar{\tau}_{\mathbf{q},\alpha})]. \end{aligned} \quad (47)$$

By using the inverse transformation (40) this can now be converted to the eigenvectors Γ . The dynamical spin correlation function of the spin liquid thus consists of two components: First, there is a two-particle continuum, which dominates for momenta around $(0, 0)$. Second, there is a single-particle like contribution, which dominates the cross section for momentum transfers near (π, π) , and hence should be identified with the excitations seen in neutron scattering around this momentum. The situation is the same for ladders, where the single-particle

spectrum is observable in the channel with momentum transfer perpendicular to the ladder, $k_\perp = \pi$, and the two-particle continuum for $k_\perp = 0$ [9].

Next, we discuss the relationship between condensation of triplets and antiferromagnetic ordering. The operator of staggered magnetization (which is a *vector*) can be written as

$$\begin{aligned} \mathbf{M}_s = & \sqrt{2N} \frac{\kappa}{4} \sqrt{\frac{n}{n_1}} \sum_{\alpha=x,y} (\bar{\tau}_{\mathbf{Q},\alpha}^\dagger + \bar{\tau}_{\mathbf{Q},\alpha}) \\ = & \sqrt{2N} \frac{\kappa}{4} \sqrt{\frac{n}{n_1}} \sqrt{2 + \chi(2)} (\bar{\tau}_{\mathbf{Q},+}^\dagger + \bar{\tau}_{\mathbf{Q},+}). \end{aligned} \quad (48)$$

Here we have used the fact that for the high-symmetry momentum \mathbf{Q} the overlap and Hamilton matrix are trivially diagonalized by the symmetric and antisymmetric combinations of the bonds in x and y -direction, $\bar{\tau}_{\mathbf{Q},\pm}^\dagger = \frac{1}{\sqrt{2}} (\bar{\tau}_{\mathbf{Q},x}^\dagger \pm \bar{\tau}_{\mathbf{Q},y}^\dagger)$. Then, introducing the 3D unit vector Ω , we can construct the coherent state

$$|\Psi_\lambda\rangle = e^{\lambda \sqrt{N} \Omega \cdot \bar{\tau}_{\mathbf{Q},+}^\dagger} |RVB\rangle.$$

This state corresponds to a condensate of the $\bar{\tau}_{\mathbf{Q},+}^\dagger$ Bosons, whose density is given by $\delta_Q = \lambda^2$. The staggered magnetization per site is

$$\mathbf{m}_s = \frac{\kappa}{2} \sqrt{\frac{\delta_Q n (1 + \chi(2)/2)}{n_1}} \Omega.$$

Inserting the value for the condensate density δ_Q obtained from (44) we obtain the value $m_s = 0.25$. Most current estimates for the 2D Heisenberg antiferromagnet are around $m_s = 0.35$ [24].

As mentioned above, the identification of antiferromagnetic ordering and condensation of some kind of effective Bosons is quite reminiscent of the treatment of Hirsch and Tang [22] in the framework of Schwinger-Boson mean-field theory [23]. In the present theory the direction of the staggered magnetization is given by the unit vector Ω , which can be chosen arbitrarily. Condensation of the triplet Bosons determines the total density of triplets, but not their distribution over the three spin species. The ‘ground state’ thus is actually an entire manifold of states which can be transformed into one another via $SO(3)$ rotations of the vector Ω . One might thus conjecture the existence of low-energy states where the direction of Ω changes slowly in real space. These states, which corresponds to a slow fluctuation of the antiferromagnetic order parameter may be describable in terms of a nonlinear σ -model - we defer a detailed discussion of this issue to a separate paper.

To conclude this section, we discuss the relationship with Zhang’s $SO(5)$ symmetric theory of cuprate superconductivity [15]. The preceding discussion has shown that an antiferromagnetic state can be viewed as a spin liquid where the triplet-like bond Bosons have condensed

into the state which has momentum (π, π) and s -like symmetry under point group operations. The antiferromagnetic order parameter, a real 3-vector, then is the vector of condensation amplitudes of the three bond-Boson species. This interpretation of the antiferromagnetic state in fact is a key ingredient for a microscopic interpretation of Zhang's SO(5) theory of cuprate superconductor. Namely the π -operator, which acts as the 'ladder operator in charge direction' in Zhang's representation of the SO(5) angular momentum algebra [15], precisely converts an s -like combination of bond triplets with momentum (π, π) into a nearest neighbor d -wave hole pair. This can be seen by writing the π -operator in real space:

$$\pi_z = \sum_i e^{i\vec{Q} \cdot \vec{R}_i} [(c_{i,\uparrow} c_{i+\hat{x},\downarrow} + c_{i,\downarrow} c_{i+\hat{x},\uparrow}) - (c_{i,\uparrow} c_{i+\hat{y},\downarrow} + c_{i,\downarrow} c_{i+\hat{y},\uparrow})]. \quad (49)$$

Introducing a further bond Boson h^\dagger , which stands for the hole pair, this could be written as

$$\pi = h_{\mathbf{K},x}^\dagger \bar{\tau}_{\mathbf{Q},x} - h_{\mathbf{K},y}^\dagger \bar{\tau}_{\mathbf{Q},y},$$

where the momentum $\mathbf{K} = (0, 0)$. Acting with $(\Omega \cdot \pi)^{\rho_N}$ onto an undoped state with the triplet condensate densities ρ_Ω will therefore convert this state into a condensate of d -like nearest neighbor hole-pairs with momentum $(0, 0)$. Viewed in this way, the connection between the antiferromagnetic and the superconducting state appears quite natural. The only drawback would be that the hole pairs are strictly nearest-neighbor pairs, i.e. the present version of the π -operator neglects charge fluctuations.

VII. DISCUSSION

In summary, we have discussed the excitation spectrum of a completely disordered and homogeneous spin system. Thereby we used an approach which might be viewed as a generalization of spin wave theory: whereas spin wave theory describes fluctuations around a Néel ordered 'vacuum', we have instead used the nearest neighbor RVB state as basis for self-consistently constructing the excitation spectrum. This general idea of treating a completely disordered state is probably more widely applicable, for example to treat the 'orbital liquids' proposed recently [26] for manganates.

As a first key result, we then found that the elementary excitations of the singlet soup-like vacuum are not Fermionic 'spinons', but rather Bosonic excitations τ_i , which can be viewed as excited dimers propagating through the system while constantly resonating between x and y direction of the dimer. Following a similar procedure as in the Zhang-Rice derivation of the t-J model,

we could write down a Hamiltonian for these Bosonic excitations. The Hamiltonian contains an energy of formation for the triplets, a term describing their propagation and a term describing pair creation and annihilation. All quantities in the derivation are quite well-defined, and can in principle be obtained by numerical techniques. In the present work we have actually attempted an 'ab initio calculation' of the various parameters in the effective Hamiltonian - a promising alternative to this somewhat clumsy approach might be a semi-empirical approach, where the parameters in the Hamiltonian are adjusted to match e.g. experimental data.

The obtained ground state is an exact spin singlet, translationally invariant and isotropic - in short, it has precisely the symmetry properties expected for a spin liquid. The elementary excitations is a triplet mode, which reaches its lowest energy at $\mathbf{Q} = (\pi, \pi)$. Such a triplet mode is the most natural generalization of an antiferromagnetic spin-wave to the spin-liquid state. Condensation of these bond Bosons into the state with momentum (π, π) then corresponds to antiferromagnetic ordering of the system. The breaking of rotational symmetry in spin space is due to fixing (different) condensation amplitudes for the three components of the triplet mode. The latter correspond to the three possible components of the antiferromagnetic order parameter.

In the present work we have chosen the completely isotropic nearest neighbor RVB-state as the starting point for constructing the triplet-Hamiltonian. This is appropriate for an truly isotropic system, which probably is realized at finite doping and/or sufficiently high temperature. Using a translationally invariant state, however, is not mandatory. For example by redefining the operator S as

$$S = \sum_i ((1 + \epsilon) s_{i,i+\hat{x}}^\dagger + (1 - \epsilon) s_{i,i+\hat{y}}^\dagger), \quad (50)$$

with $\epsilon > 0$ we can obviously generate a 'singlet soup' with a preference for singlet orientation in x -direction. It is tempting to speculate that this may be appropriate for orthorhombic $\text{La}_{1-x}\text{Sr}_x\text{CuO}_4$, where at $x = 0.125$ columnar order is known to exist. Analogous calculation as above, but with a finite ϵ may thus be appropriate to discuss the excitation spectrum of this material.

Finally we note that the present scenario for the excitation spectrum of the spin-liquid provides a corner stone for a microscopic interpretation of Zhang's SO(5) symmetric theory of cuprate superconductors [15]. As discussed above, an antiferromagnetic state may be thought of as being generated by condensing triplet-like spin excitations of the RVB spin-liquid into the state with momentum (π, π) . The antiferromagnetic order parameter corresponds to the vector of condensation amplitudes of the three triplet species. Then, SO(5) symmetry states that such a triplet-excitation with momentum (π, π) is 'dynamically equivalent' to a $d_{x^2-y^2}$ hole pair [25]. In

fact the π -operator [15], which plays the role of a ladder operator for ‘rotations in charge-direction’ in the SO(5) theory [15], precisely replaces a bond-triplet with momentum (π, π) by a hole pair with momentum $(0, 0)$. The fact that the π -operator is an approximate eigenoperator of the Hamiltonian, $[H, \pi] = \omega_0 \pi$, then implies that the triplet and the hole pair are dynamically indistinguishable and differ only by their energy of formation. The π -operator thus would convert a condensate of triplets into a condensate of hole pairs, and, by the dynamical equivalence of these two objects, thus converts the anti-ferromagnetic ground state at half-filling into a superconducting state at finite-doping one. The somewhat ‘toy-model-type’ discussion of Ref. [25] thus may very well be transferable almost literally to the fully planar t-J model. In the present work we have restricted ourselves to a pure spin system. One may expect, however, that all considerations go through also for the doped system, with the sole difference that we get additional renormalizations of the matrix elements in the effective Hamiltonian due to the fact that the doped holes reduce the volume available for pair generation and propagation of triplets. Moreover, we will need terms which describe the coupling of the triplet branch to the mobile holes. In the simpler case of hole motion in a spin ladder this program has in fact already been carried out [9,27], leading to quite satisfactory agreement with numerical results. For the planar case we defer this to future work.

I would like to thank W. Hanke, O. P. Sushkov and Shou-Cheng Zhang for instructive discussions and helpful comments.

VIII. APPENDIX

In this appendix we discuss the numerical work needed to obtain the values of $\chi(u)$, $\epsilon_0(u)$ and the η . To that end all possible dimer coverings of an $M \times M$ cluster with periodic boundary conditions are generated on the computer the sums in (13) are evaluated numerically. Restrictions on computer memory and CPU time do not allow to use $M > 6$, so that in practice only $M = 4, 6$ are possible. To study the size dependence, we consider the quantities $\bar{\chi}(L) = \frac{n_1}{n} \chi(L)$; these give the ratio of the norm of an RVB state covering the exterior of a loop of length L to the norm of an RVB state covering the entire cluster. Similarly, we define $\bar{\epsilon}_0(L) = \frac{n_1}{n} \epsilon_0(L)$, which gives the gain or loss in energy due to a fixed loop of length L . The values for the different $\bar{\chi}$ and $\bar{\epsilon}_0$ are given in Table I and actually show already a quite remarkable independence of systems size. Moreover, the expectation value of the energy/bond, E_0/N , is -0.334318 for $M = 4$, -0.313763 for $M = 6$; the estimate for $L = \infty$ is -0.302 [16]. All in all the data suggest that already the 4×4 cluster gives reasonably accurate estimates for the different parameters.

Moreover, the data show that the $\bar{\chi}(L)$ and $\bar{\epsilon}_0(L)$ decrease quite rapidly with L . truncation of the series after $L = 2$ thus seems to be quite a reasonable approximation as well.

L	M=2		M=4	
	$\bar{\chi}(L)$	$\bar{\epsilon}_0(L)$	$\bar{\chi}(L)$	$\bar{\epsilon}_0(L)$
1	0.10953	0.13844	0.121483	0.15142
2	0.03602	0.01675	0.043671	0.01998
3	0.00780	-0.00197	0.012879	-0.00001

TABLE I. The values of $\bar{\chi}(L)$ and $\bar{\epsilon}_0(L)$ for the two different L .

-
- [1] S. Kivelson, D. Rokhsar, and J. P. Sethna, Phys. Rev. B **35**, 865 (1987).
- [2] B. Sutherland, Phys. Rev. B **37**, 3786 (1988).
- [3] M. Kohmoto, Phys. Rev. B **37**, 3812 (1988).
- [4] E. Fradkin, *Field Theories of Condensed Matter Systems*, Addison-Wesley Publishing Company, 1991.
- [5] P.W. Kasteleyn, Physica **27** (1961) 1209.
- [6] S. Sachdev and R. N. Bhatt, Phys. Rev. B **41**, 9323 (1990).
- [7] R. R. P. Singh, M. P. Gelfand, and D. A. Huse, Phys. Rev. Lett. **61**, 2484 (1988).
- [8] S. Gopalan, T. M. Rice, and M. Sigrist, Phys. Rev. B **49**, 8901 (1994).
- [9] R. Eder, Phys. Rev. B **57**, 12823 (1998).
- [10] A. V. Chubukov and D. K. Morr, Phys. Rev. B **52**, 3521 (1995).
- [11] V. N. Kotov, O. Sushkov, Zheng Weihong, and J. Oitmaa, Phys. Rev. Lett. **80**, 5790 (1998).
- [12] Han-Ting Wang, Jue-Lian Shen, and Zhao-Bin Su, Phys. Rev. B. **56**, 14435, (1997).
- [13] W. Brenig, Phys. Rev. B. **56**, 14441, (1997).
- [14] R. Eder, O. Stoica, and G. A. Sawatzky, Phys. Rev. B. **55**, 6109, (1997); R. Eder, O. Rogojanu, and G. A. Sawatzky, Phys. Rev. B. **58**, 7599, (1998).
- [15] S.C. Zhang, Science **275**, 1089 (1997).
- [16] S. Liang, B. Doucot, and P. W. Anderson, Phys. Rev. Lett. **61**, 365 (1988).
- [17] A. V. Chubukov, JETP Lett. **49**, 129 (1989).
- [18] It should be noted that by defining the states

$$|\Psi_{i_1, \sigma_1, i_2, \sigma_2, \dots, i_m, \sigma_m}\rangle = \frac{S^{N-m/2}}{(N-m/2)!} \prod_{\nu=1}^m \hat{c}_{i_\nu, \sigma_\nu}^\dagger |0\rangle,$$

one could also construct a basis of ‘spinon’ states and re-interpreting

$$|\psi_{i_1, \sigma_1, i_2, \sigma_2, \dots, i_m, \sigma_m}\rangle \rightarrow \prod_{\nu=1}^m a_{i_\nu, \sigma_\nu}^\dagger |0\rangle,$$

where the $a_{i_\nu, \sigma_\nu}^\dagger$ now correspond to spin-1/2 Fermions one might be tempted to try and derive a *Fermionic* Hamiltonian for the ‘spinons’:

$$H = \sum_{i,j} \epsilon_{ij} a_{i,\sigma}^\dagger a_{j,\sigma}, \\ + \sum_{i,j} (\Delta_{ij} a_{i,\sigma}^\dagger a_{j,\bar{\sigma}}^\dagger + H.c.)$$

Readers uncomfortable with the triplet excitation picture put forward in this work are invited to try their hands on this calculation - the present author trusts that this experience will convince anybody that the triplets are the one and only sensible way of discussing the excitation spectrum of the spin liquid.

- [19] G. Stollhoff and P. Fulde, J. Chem. Phys. **73**, 4548 (1980).
- [20] F. C. Zhang and T. M. Rice, Phys. Rev. B **37**, 3759 (1988).
- [21] T. Ogawa, K. Kanda, and T. Matsubara, Progr. Theor. Phys. **53**, 614 (1975); see also D. Vollhardt, Rev. Mod. Phys. **56** 99 (1984).
- [22] J. E. Hirsch and S. Tang, Phys. Rev. B **39**, 2850 (1989).
- [23] D. P. Arovas and A. Auerbach, Phys. Rev. B **38**, 316 (1988).
- [24] E. Manouskais, Rev. Mod. Phys. **63**, 1 (1991).
- [25] R. Eder, A. Dorneich, M. G. Zacher, W. Hanke, and Shou-Cheng Zhang, preprint cond-mat/9805120.
- [26] L. F. Feiner, A. M. Oles, and J. Zaanen, Phys. Rev. Lett. **78**, 2799 (1997).
- [27] O. P. Sushkov, preprint cond-mat/9808302.